Looking into the Progenitor of Supernova Remnant N157B with Chandra

Elvira Cruz-Cruz[1,2], Laura A. Lopez[1,2], Jennifer A. Rodriguez[1,2], Katie Auchettl[3,4], & Tyler Holland-Ashford[5]

[1]Department of Astronomy, The Ohio State University
[2]Center for Cosmology and AstroParticle Physics, The Ohio State University
[3]School of Physics, University of Melbourne, Parkville, VIC 3010, Australia
[4]Department of Astronomy and Astrophysics, University of California, Santa Cruz, CA, USA
[5]Astrophysics Science Division, NASA Goddard Space Flight Center Greenbelt, MD, USA

On the postdoc job market Fall 2026

SCAN ME

1 Motivation

Understanding SNe progenitor properties, their relation to SNe and remnants, is essential for:

- Understanding the death of massive stars
- Exploring the role of binaries
- Investigating the origins of merging systems that produce gravitational waves

In core-collapse SNe (ccSNe):

- The explosion can leave behind a supernova remnant and a compact object (neutron star or black hole)
- Remnants serve as observational probes of massive star evolution, supernova mechanisms, and compact object formation

Chemical composition of the ejecta reveals nucleosynthesis from the explosion:

- CCSNe primarily produce alpha-elements (O, Ne, Mg, Si, S)
- Chemical abundance ratios are proportional to zero-age main-sequence (ZAMS) progenitor mass, as shown in nucleosynthesis yield models (e.g., Sukhbold et al. 2016)

Advantages of studying N157B:

- Known explosion outcome (neutron star), contains a fast pulsar PSR J053747.39-691020.2, which powers a bright, nonthermal X-ray nebula (visible in hard X-rays)
- Deep 2 Ms of Chandra X-ray observations available
- Located in 30 Doradus (star-forming region) -> insights into the progenitor nature
- Strong X-ray thermal emission from the supernova ejecta enables quantification of metal abundances in the plasma around the PWN
- Chen et al. (2006) found metal-enriched ejecta in N157B with 48ks Chandra observations & estimated the progenitor mass to be ≥20 $M_{\odot}$ using X-ray thermal emission analysis

Chandra Observations

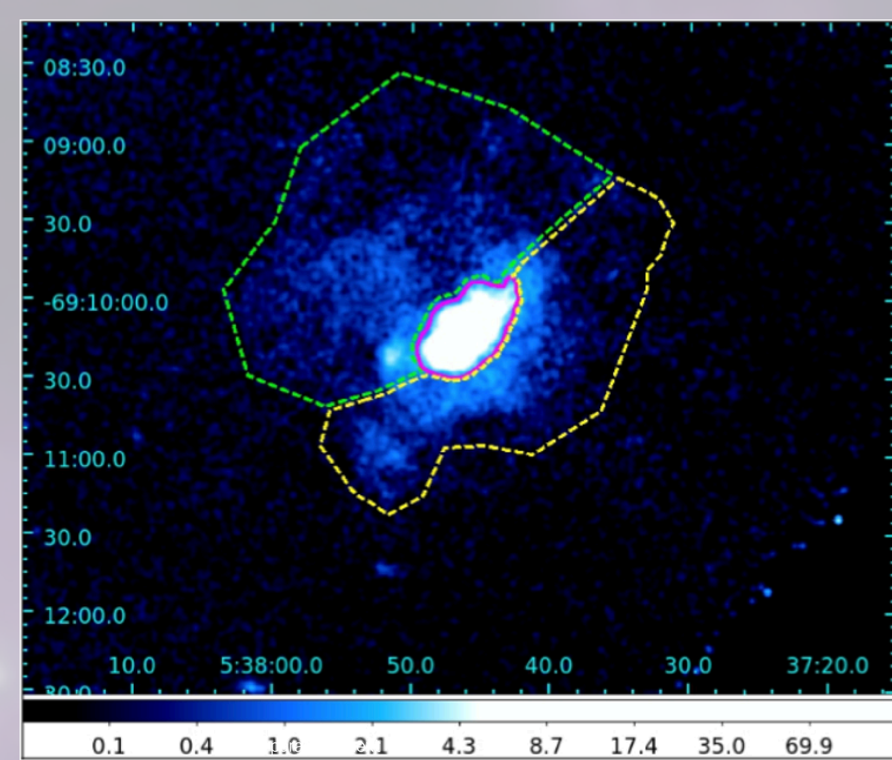

Figure 1: Combined Chandra X-ray (blue) broad image, 0.5-7.0 keV, no point-source subtraction. Northern region encompasses the green polygon region, north of the pulsar wind nebula (PWN). The southern region is shown in yellow. The PWN is the magenta central region, and is not included in the spectral analysis,

2 Methodology

Leisa Townsley's 2 Ms X-ray Visionary Project of 30 Doradus covered N157B with Chandra.

- Extract X-ray spectra from 35 Chandra observations (2 Ms total) using CIAO to study the thermal diffuse emission of the supernova ejecta surrounding the PWN
- Define two polygon regions: North (>14,000 counts) and South (>10,000 counts) of the PWN (Fig. 1)
- Fit background-subtracted spectra with XSPEC model: const × phabs × vphabs × (powerlaw + vpshock)
  - Galactic absorption frozen: $N_H = 0.0644 \times 10^{22}$ cm^{-2}
  - LMC absorption free to vary: $N_H = 0.504 \times 10^{22}$ cm^{-2}, metals frozen at 0.5 $Z_{\odot}$
  - vpshock (NEI): O, Ne, Mg, Si are free; other abundances frozen at 0.5 $Z_{\odot}$. Power-law photon index frozen at 2.3 (Chen et al. 2006)

Convert XSPEC abundance fits to ejecta masses ($M_{\odot}$):

- Convert abundances (O, Ne, Mg, & Si) using the XSPEC normalization, LMC distance (50 kpc), emitting volume (total volume x filling factor), and Asplund et al. (2009) solar abundances; (Holland-Ashford et al. 2023)
- Compare observed ratios to Sukhbold et al. (2016) CCSNe nucleosynthesis yield models using three explosion engines:
  - N20 & W18: 12.5–120 $M_{\odot}$; Z9.6: 9–12 $M_{\odot}$
- Evaluate Gaussian log-likelihood at each discrete model grid mass; best fit = max. likelihood; $\Delta\ln\mathcal{L} \geq -0.5$ (1σ), $\Delta\ln\mathcal{L} \geq -2.0$ (2σ)

X-ray Spectral fitting

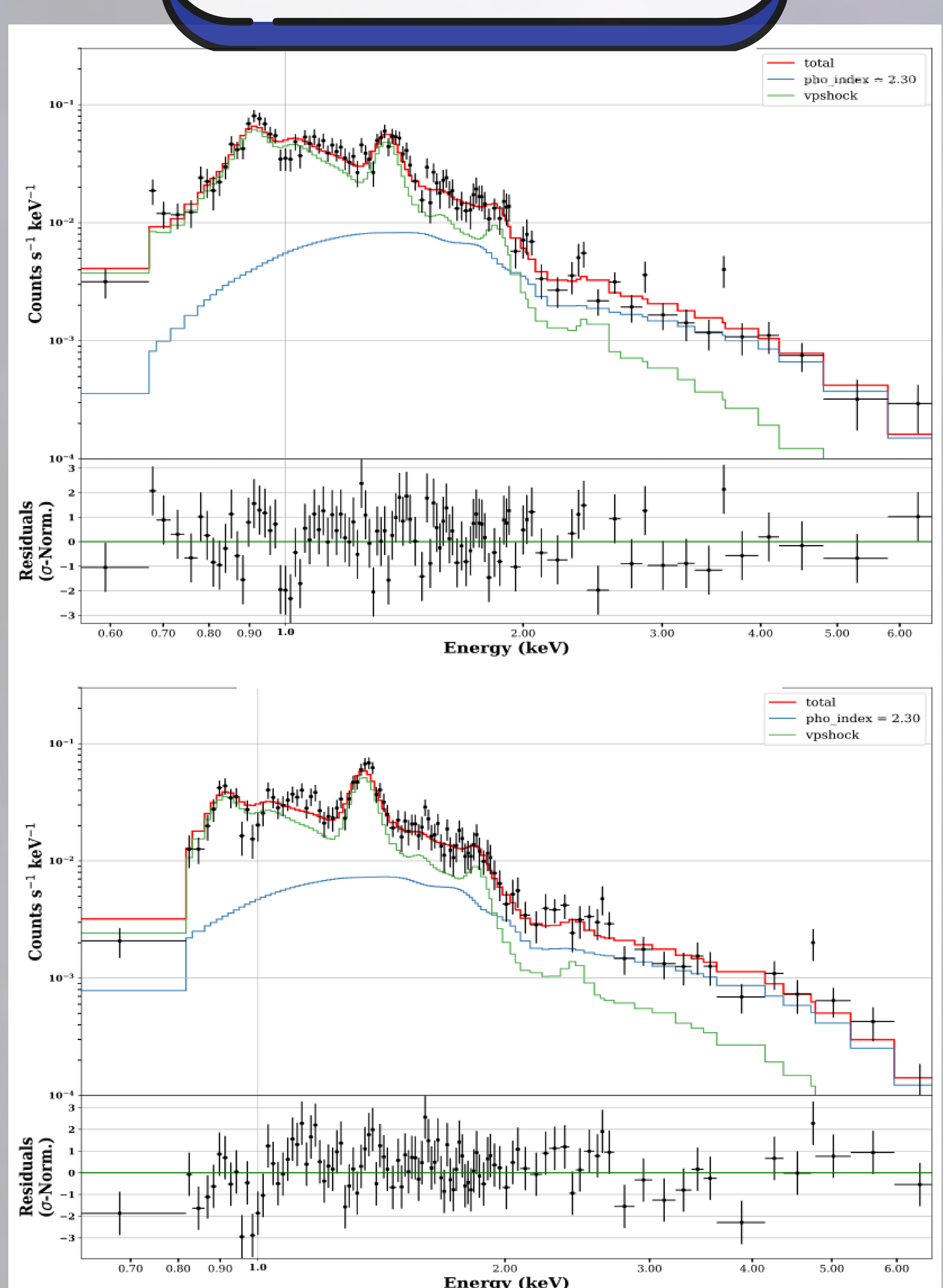

Figure 2: Background-subtracted spectra of the northern (top) and southern region (bottom) from the deepest, 94 ks, observation, 16192, with the total spectral model fit, separate model components, and residuals plotted. The thermal (non-thermal) emission dominates below <2 keV (>2 keV). The spectral thermal component is fit with the XSPEC vpshock model, and the non-thermal is fit with an added power-law.

3 Spectral Results & Models

Below: The table shows the spectral model fit results of the abundances, plasma temperatures, column density, and ejecta's ionization timescale.

Table 1. Spectral fit of the northern and southern regions.

Parameter	North	South
$N_H^{LMC}(\times 10^{22}\mathrm{cm}^{-2})$	$0.83^{+0.08}_{-0.13}$	$2.31^{+0.15}_{-0.09}$
kT(keV)	$1.37^{+0.22}_{-0.09}$	$0.68^{+0.036}_{-0.045}$
$\mathrm{O/O}_{\odot}$	$0.71^{+0.17}_{-0.18}$	0.5
$\mathrm{Ne/Ne}_{\odot}$	$1.75^{+0.26}_{-0.19}$	$1.54^{+0.135}_{-0.128}$
$\mathrm{Mg/Mg}_{\odot}$	$1.158^{+0.17}_{-0.09}$	$0.96^{+0.074}_{-0.039}$
$\mathrm{Si/Si}_{\odot}$	$0.52^{+0.10}_{-0.06}$	$0.33^{+0.042}_{-0.037}$
$n_e t\ (\times 10^{10}\mathrm{s/cm^3})$	$4.45^{+0.47}_{-0.59}$	$6.72^{+10.06}_{-9.903}$
χ^2/dof	5085/4910 = 1.03	4533/4269 = 1.06

Northern and Southern Spectral Fit Results:

- **Both regions have ionization timescales $n_e t < 10^{11}$ s cm^{-3}**
  - The shock-heated ejecta surrounding the PWN is still in non-equilibrium ionization (NEI).
- O, Ne, and Mg are higher than the ISM (0.5 $Z_{\odot}$) metallicity
  - indicating a very metal-rich ejecta dominated by diffuse thermal emission
- The PWN near the center of the remnant contributes to the X-ray spectra at higher energies (> 2 keV) and doesn't dominate the spectra at lower energies (Fig. 2).

The NEI state of the ejecta, the detection of high O, Ne, and Mg, and the presence of a pulsar indicate the remnant is young and is the outcome of a ccSNe.

The Sukhbold et al. (2016) Nucleosynthesis Yield Models:

- CCSNe nucleosynthesis yields for a grid of 9–120 $M_{\odot}$ progenitors using a 1D neutrino-driven explosion model calibrated to observed SNe
- Three neutrino-driven engines calibrated to observed SNe:
  - **N20**: calibrated to SN 1987A using a 20 $M_{\odot}$ blue supergiant progenitor; covers 12.5–120 $M_{\odot}$
  - **W18**: calibrated to SN 1987A using a rotating 18 $M_{\odot}$ blue supergiant progenitor; intermediate engine; covers 12.5–120 $M_{\odot}$
  - **Z9.6 (9.6$M_{\odot}$ zero-metallicity model by A. Heger)**: calibrated to the Crab Nebula; covers 9–12 $M_{\odot}$
- Yields vary irregularly with progenitor mass, reflecting whether each star successfully explodes or implodes
- We use the dominant stable isotope of each element: ^{16}O, ^{20}Ne, ^{24}Mg, ^{28}Si, and the production yields of stars that explode.

4 Comparing Abundance Mass Ratios to Nucleosynthesis Yield Models

Figure 3: $\Delta\ln\mathcal{L}$ as a function of progenitor mass for the N20 (left) & W18 (right) explosion models from Sukhbold et al. (2016). The red vertical line marks the best-fit progenitor mass. The dashed & dotted horizontal lines (shaded regions) indicate the 1σ and 2σ confidence thresholds (mass range).

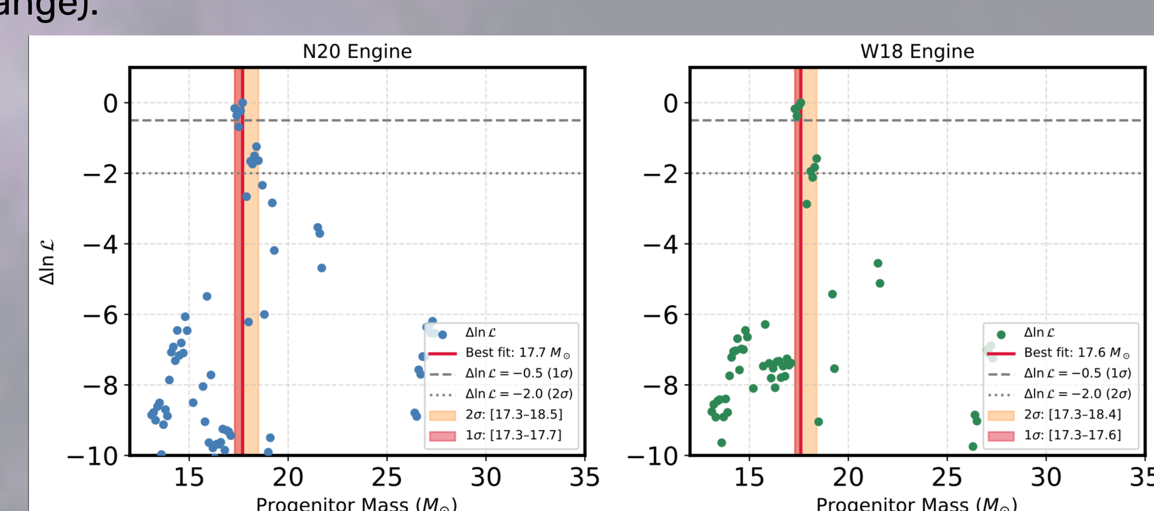

Fig. 3 (above) shows the log-likelihood at each Sukhbold et al. (2016) grid mass for N20 and W18 engines with confidence intervals:

- **N20:** 17.7 $M_{\odot}$, 1σ = 17.3$M_{\odot}$–17.7$M_{\odot}$, 2σ = 17.3$M_{\odot}$–18.5$M_{\odot}$
- **W18:** 17.6 $M_{\odot}$, 1σ = 17.3$M_{\odot}$–17.6$M_{\odot}$, 2σ = 17.3$M_{\odot}$–18.4$M_{\odot}$
- The agreement between two independent explosion engines strengthens the progenitor mass estimate.

Fig. 4 (below) shows the observed [X/Si] ratios (black points) overlaid with the respective model predictions from Sukhbold et al. (2016) at the best-fit mass. The shaded bands show the spread of model predictions across the 1σ and 2σ confidence intervals.

- [Mg/Si] shows some agreement with N20 & W18 predictions; [O/Si] and [Ne/Si] show tension, likely driven by frozen South O abundance and systematic uncertainties in emitting volume

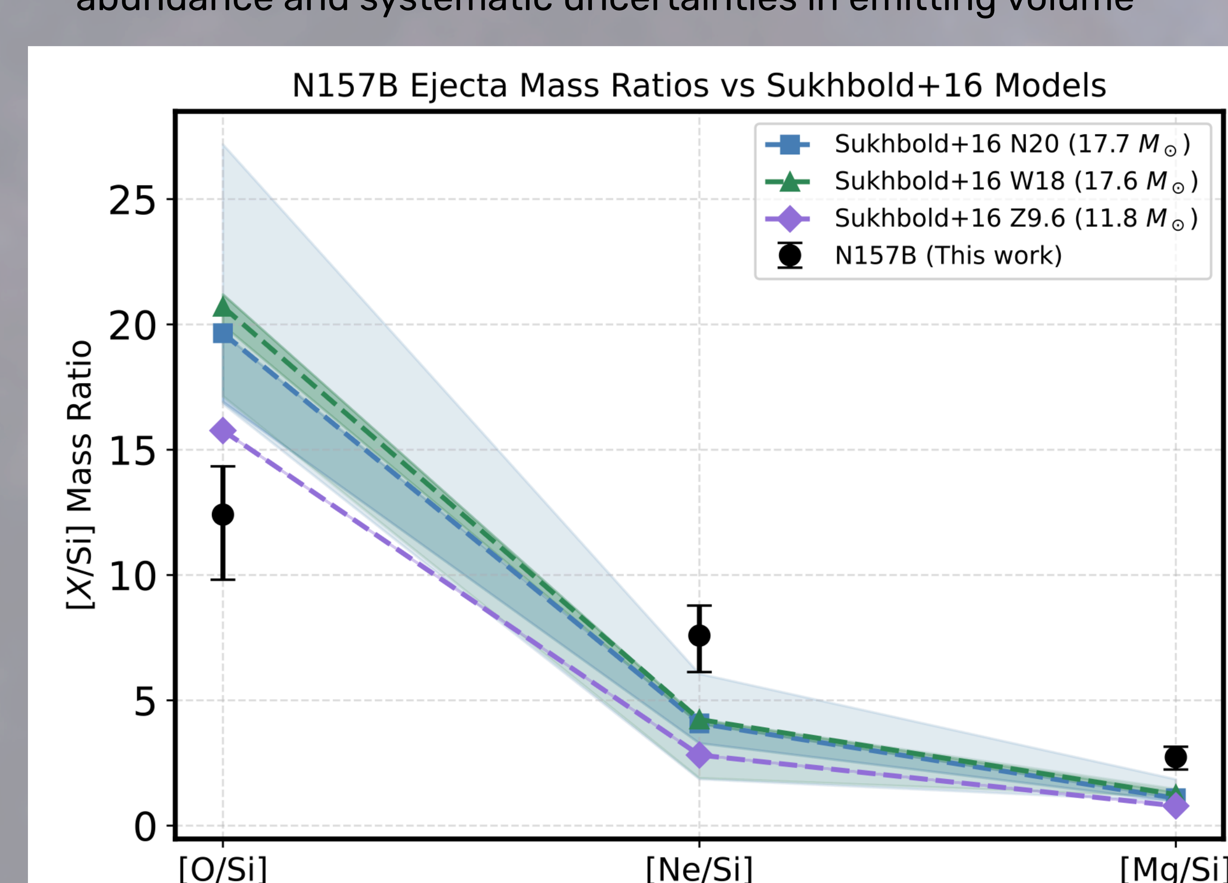

Figure 4: The observed total ejecta mass ratios [X/Si] for N157B (black points with asymmetric 1σ error bars) compared to Sukhbold et al. (2016) model predictions at the best-fit progenitor mass for each engine. The shaded bands show the spread of model [X/Si] results across the 1σ and 2σ confidence intervals. [Mg/Si] shows broad agreement with the N20 and W18 model results at ~17–18 $M_{\odot}$.

5 Conclusions & Outlooks

- N157B ejecta surrounding the PWN is metal-rich and in NEI, consistent with a young core-collapse SNR
- Best-fit progenitor mass: ~17–18 $M_{\odot}$ (N20 & W18 engines), broadly consistent with Chen et al. (2006)
- Z9.6 engine disfavored, since observed ratios require progenitor mass above its 9–12 $M_{\odot}$ grid
- Observed [Mg/Si] consistent with model predictions; [O/Si] and [Ne/Si] show some remaining tension
- Next steps: refine emitting volume assumptions, explore other filling factor assumptions